www.sciencetranslationalmedicine.org/cgi/content/full/5/191/191ra84/DC1

Supplementary Materials for

Identifying the Interaction Between Influenza and Pneumococcal Pneumonia Using Incidence Data

Sourya Shrestha,* Betsy Foxman, Daniel M. Weinberger, Claudia Steiner, Cécile Viboud, Pejman Rohani

*Corresponding author. E-mail: sourya@umich.edu

Published 26 June 2013, *Sci. Transl. Med.* **5**, 191ra84 (2013)
DOI: 10.1126/scitranslmed.3005982

The PDF file includes:

S-1 Additional Results

S-1.1 Epidemiology of pneumococcal pneumonia

As we infer the interaction between influenza and pneumococcal pneumonia, we indirectly make some inference of the pneumococcal epidemiology. Instead of relying on *a priori* estimates, we have directly estimated them within the proposed modeling framework, giving us a sense of an epidemiological regime that the data directly points to. MLEs for data set I and data set II are provided in Table S-3.3.

In both data sets, we find the role of carriage to be important, seen in the non-zero values for ω in the MLE estimates. Additionally, we constructed a likelihood profile of ω, the contribution of carriage to the total force of infection, in data set II, which is presented in Fig. S2[Left]. The precipitous drop in likelihood scores for low values of ω shows that it is an essential component of the model. We further estimate the fractional contribution of ω to the total force of infection, via simulations of the MLE models. We find that the contribution of ω to the pneumococcal hazard, $[(\omega)/(I/N + \omega)]$, on average over the length of the data to be 93.82% and 94.99% in data set I and data set II, respectively. This suggests that carriage is the primary driver of the pneumococcal epidemiology. Although it is unclear how the carriage affects invasive pneumococcal pneumonia, it is thought of to be an important factor [35,36,37]. It is also believed that a substantial fraction of the population can be carrying pneumococcal bacteria in the naso-pharynx without showing any symptom [36,43]. In this regard, our findings are more or less consistent with the prevailing thought in the literature.

We find the average length of pneumococcal infection to be about 4.8 days and 4.0 days in data set I and data set II, respectively. This should be taken with caution when directly comparing with pneumococcal infections in hospitalized patients. Pneumococcal infections can last longer in general, and our estimate may be shorter for several reasons. First, pneumococcal infections may vary widely in their duration. In particular, the ones that are not reported may be shorter that those that are reported. Hence, estimates based on clinical or hospitalized cases may find a longer duration of the infection. Second, from the model's perspective, the estimate is of the average length that an individual is infectious rather than average length of the infection itself. Symptoms of the infection may persist past the point where the individual is infectious, or the individual may not be actively contributing to the transmission because the individual is at a hospital or resting.

We find low rates of reporting for pneumococcal pneumonia-the MLE estimates for the reporting ratios were 2.4% in data set I and 0.1% in data set II. We interpret this to be indicative of two things. First, the hospitalization data are of severe cases, and are hence expected to be a gross underestimate of total cases. Second, the model suggests high abundance of asymptomatic pneumococcal pneumonia. Additionally, we found this reporting ratio to be considerably lower in data set II compared to data set I. One interpretation of this reduction is that although pneumococcal vaccine reduced the reported cases, the overall abundance of pneumococcal pneumonia were not reduced. The pneumococcal conjugate vaccine introduced in 2000, targeted only 7 out of 92 pneumococcal serotypes that were disproportionately associated with pneumococcal pneumonia. Risk of pneumococcal pneumonia is serotype dependent, and furthermore, it has been suggested that carriage rates and pneumococcal risk may be inversely related, i.e. serotypes that are associated with higher pneumococcal risk are relatively inefficient colonizer, and *vice versa* [37]. This scenario is consistent with the idea that pneumococcal vaccine may induce rapid serotype replacement [44], and furthermore the replacing serotypes may be inferior to the previously circulating serotypes in causing pneumococcal pneumonia [37]. Hence, one would see decrease in the incidence of pneumococcal pneumonia, but no decrease or even an increase in carriage rates. Further targeted research is necessary to conclusively establish this claim.

The seasonality in the transmission is captured by βs in the model. We find the transmission to be approximately two to three times as high during high part of the season compared to low part of season. The differences in the rates between data set I and data set II are again reflective of higher prevalence of

asymptomatic pneumococcal pneumonia in the post-PCV7 era. The model also allows for loss of immunity, and the duration of the immunity was estimated to be around 10 years in both data sets. Given that the data sets were themselves 8-10 years, we take this as only an absence of a shorter term immune dynamics in the pneumococcal pneumonia. However, it should be noted that we allow for carriage to be present at a constant level in our model. This formulation will by itself include any role loss immunity might play in the maintenance of constantly high carriage. Hence an alternative formulation is required for a proper inference of the duration of immunity.

We also rely on the inference of the reporting ratios of influenza to infer the interaction. We find this reporting ratio to be similar in both data sets, at around 1%. We additionally constructed a likelihood profile for ρ_F in data set II, which is presented in Fig. S2[Right]. It is important to note that this estimate is based solely on the influenza-pneumococcal interaction model, and not on influenza dynamics itself. Nonetheless, this estimate is in a similar range to the reporting ratios estimated during 2009 pandemic-1/222 cases are hospitalized [45,46], or 1.44% of all symptomatic cases are hospitalized [47].

S-1.1.1 Model simulations

Given our estimates, we can directly compare the predictions borne out from the models with the data. We simulate the MLE and null models for each data set 1000 times to generate means and 95% confidence intervals. The simulations of the MLE models in comparison to the null models are shown in Figs. S3, and S4, for data set I and data set II, respectively. As discussed in the main text, these results show that although null models can capture seasonal patterns in pneumococcal pneumonia cases, they fail to capture the interannual variability in the peaks. Accounting for influenza as a factor of susceptibility enhancement enables us to explain this variability. This can also be seen in the improvement in the R^2 goodness of fit measures that MLE models achieve over null models (See Fig. S5).

S-1.2 Timescale of the interaction

In the original model, we hypothesized that individuals currently or very recently infected (up to a week) with influenza face different hazard rate compared to those that do not. Here, we hypothesize that individuals infected up to three weeks in the past with influenza face different hazard rates. Let $F_1(t)$, and $F_2(t)$ respectively be the influenza case reports 1 week and 2 weeks in the past, i.e. $F_1(t) = F(t–1)$, and $F_2(t) = F(t–2)$. Let S_{F1}, and S_{F2} respectively be the sizes of the susceptible population that were infected with influenza between 1-2 weeks, and 2-3 weeks in the past. We estimate these quantities in the same way we estimated S_F. i.e., $S_{F1} = [(F_1(t))/(\rho_F N)]\, S$, and $S_{F2} = [(F_2(t))/(\rho_F N)]\, S$. With S_F, defined the same way as in the original model, and S_U being the rest of the susceptible population, the susceptible compartment is now divided into 4 sub-compartments: S_F, S_{F1}, S_{F2}, and S_U. Let the hazard rates faced by each of the susceptible sub-compartments be $\phi\,\lambda$, $\phi_1\,\lambda$, $\phi_2\,\lambda$, and λ, respectively. The complete lagged-interaction model is described by the following set of equations:

$$\frac{dS}{dt} = \mu(N–S) – \lambda\, S_U – \phi\,\lambda\, S_F – \phi_1\,\lambda\, S_{F1} – \phi_2\,\lambda\, S_{F2} + \varepsilon\, R$$

$$\frac{dI}{dt} = \lambda\, S_U + \phi\,\lambda\, S_F + \phi_1\,\lambda\, S_{F1} + \phi_2\,\lambda\, S_{F2} – \gamma\, I – \mu\, I$$

$$\frac{dR}{dt} = \gamma I - \mu R - \varepsilon R$$

$$S_F = \frac{F(t)}{\rho_F N} S$$

$$S_{F1} = \frac{F_1(t)}{\rho_F N} S$$

$$S_{F2} = \frac{F_2(t)}{\rho_F N} S$$

$$S_U = S - S_F - S_{F1} - S_{F2} = S - \frac{F(t)}{\rho_F N} S - \frac{F_1(t)}{\rho_F N} S - \frac{F_2(t)}{\rho_F N} S$$

Our estimates for ϕ_1 and ϕ_2, for pneumococcal pneumonia in data set II, is shown in Fig. S6. We find that the null models, $\phi_1 = 1$ and $\phi_2 = 1$ are within the 95% confidence interval, indicating that there is no evidence of susceptibility enhancement among cohorts that were infected with influenza more than 1 weeks prior.

S-2 A brief literature survey on influenza-pneumococcal interaction.

Here, we provide a sample (not meant to be exhaustive) of literature that study association between influenza and invasive pneumococcal disease, in pandemic and non-pandemic years.

S-2.1 Pandemic years

- Spanish influenza pandemic (1918-1919).
    - [10] examines lung tissues from 58 autopsies from 1918 pandemic fatalities and 8398 individual autopsy investigations from publications related to 1918 patients. They find that in virtually all 58 cases, bacterial pneumonia were either the predominant cause or played a role in the pathology. Furthermore, 20-25% cases from the published autopsy investigations recovered pneumococcal bacteria from the cultures.
    - [48] provides a historical review of interactions between influenza and pneumococci, particularly in army camps all over US during in the 1918 pandemic. It reports that on average 16% of the influenza patients also had pneumonia. In some camps, the pneumonia or deaths lagged the influenza peaks by 7-10 days.
    - [49] reports a table of influenza, and pneumonia cases from Sep 12 to Oct 31, 1918 in all the army camps.
- Asian influenza pandemic (1957-1958).
    - [15] report bacterial co-infections among 24 out of 33 patients that attended New York Hospital-Cornell Medical Center during Asian influenza pandemic of 1957-1958. 15 of the 24 were late bacterial co-infections.

    - [50] find bacteria (38 staph aureus, and 12 pneumococci) in the sputum of 69 out of 140 cases admitted to City General Hospital of Sheffield during the peak months, September and October of 1957.
    - [51] report bacteria in 24 out of 33 fatal cases (13 staph, 7 pneumococcus) from greater Cleveland area.
- Hong Kong influenza pandemic (1969-1970).
    - [16] report pneumonia complications (most with bacteria) in 20 of 127 patients that attended Mayo clinic during Hong Kong flu.
    - [52] report increase in pneumonia cases (mostly Staphylococcal pneumonia) during 1968-69 Hong Kong flu at Grady Memorial Hospital, Atlanta, compared to the year before.
    - [17] report bacteria in at least 54 of the 106 adult patients admitted to City Memphis Hospitals. Most of the bacteria were pneumococcus, and only a few staphylococcus aureus, and the low occurrence of staph was thought of as the reason for lower than expected mortality.
- Swine influenza pandemic (2009-2010).
    - [53] report 26% of the 100 fatal cases during 2009 pandemic had bacterial coinfection.
    - [54] report 8 out of 21 fatal patients in Brazil were co-infected.
    - [18] report histologic and microbiologic autopsy evidence of bacterial pneumonia was detected in 55% of 34 fatal cases.
    - [55] find that presence of *S. pneumoniae* in the nasopharyngeal swabs led to more severe disease among H1N1 patients in Argentina.
    - [11] use hospitalizations from the US State Inpatient Databases of the Healthcare Cost and Utilization Project 2003â€“2009, and find that the 2009 influenza pandemic had a significant impact on the rate of pneumococcal pneumonia hospitalizations, with the magnitude of this effect varying between age groups and states, mirroring observed variations in influenza activity.

S-2.2 Non-pandemic years

- [56] look at the association (correlation) between isolates of *S. pneumoniae* and influenza and respiratory syncytial viruses, as well as other climatic variables in 36 months of bi-weekly data from Houston, between June 1990 to May 1993. Pneumococcal isolates were either through blood or CSF; the reported number is aggregated over participating hospitals. Viral isolation was done via throat swab and nasal washing specimens collected in symptomatic patients who attended participating primary care clinics or physicians. They find that pneumococcal infections are associated with both influenza and RSV (correlation coefficient $r = 0.46$ and 0.56, respectively).
- [24] look at association between influenza and *S. pneumoniae* in 3 broadly defined US census regions (South, North-east and West) over 11 season between 1995 to 2006 (non-pandemic period). Influenza data are weekly %positive in collected samples (WHO participating labs), and pneumococcal pneumonia data are number of lab-confirmed cases (from the surveillance (ABCs)) grouped weekly, and converted to incidence (per 10 million). The authors first estimate an expected baseline for pneumococcal pneumonia in the absence of influenza, and calculate the residuals (observed - expected) - but find no significant association with the influenza reports. The authors then go on to use negative binomial regression model, find significant association at 1-week lag (for pneumococcal pneumonia), and conclude modest increases in the rates of invasive pneumococcal pneumonia during winters associated with influenza circulation.
- [25] look at positive influenza cases in Central Ontario, Canada (via a surveillance network of hospitals and laboratories) and episodes of invasive pneumococcal disease (IPD) in Toronto/Peel area (Toronto Invasive Bacterial Diseases Network) between 1995-2009. They find no correlation in the seasonality of the two epidemics, but find evidence to support influenza A and/or B Granger-cause pneumococcal infections. They also find significant association between total influenza and invasive pneumococcal disease (IPD) with 1-wk lag using a case-crossover approach. They conclude that they find no epidemiological evidence that influenza has a strong effect on invasive pneumococcal disease (IPD) risk via changes in transmission dynamics.

- [26] find no association between influenza A and IPI in Germany in children below 16 from 1997-2003.
- [57] find an annual increase of 6-10% in IPD due to influenza in Sweden during 1994-2004.
- [58] find association between respiratory syncytial virus (RSV) and invasive pneumococcal disease (IPD), but not between influenza and IPD in Australia in 2000.
- [59] find association between invasive pneumococcal disease (IPD) and influenza viruses, respiratory syncytial virus (RSV), adenovirus and parainfluenza virus 3 in New Zealand during 1995-2006. The study does not account for co-seasonality.
- [60] report correlation between IPD and RSV and influenza virus in the Netherlands during 1997-2003. The study does not account for co-seasonality.

S-3 Sensitivity analyses

S-3.1 Alternative model with vaccination

To infer the pathways of interaction, and their estimates in post-vaccine Illinois data of influenza and pneumococcal pneumonia (data set II), we originally used a model that did not model vaccine explicitly-the reasoning behind this was that a model of vaccination that does not allow for waning of vaccine derived immunity, can be rescaled to the form that does not model vaccine explicitly [61]. Here, we re-infer the susceptibility impact, using a model where the dynamic effects of vaccination is modeled explicitly. As illustrated in Fig. S7, we include an additional compartment in our model, *V* that tracks individuals that are currently protected against pneumococcal pneumonia due to vaccine-derived immunity. We assume that each new-born individual will receive an efficacious vaccine with probability ν. Only the remaining individuals that do not receive efficacious vaccine enter the susceptible class. We further assume that vaccine derived immunity can wane at a per capita rate ε_v.

Using the same inference procedure, we infer the susceptibility impact ϕ, in the absence of transmission and severity impact, ie $\theta = 1$, and $\xi = 1$. As seen in the likelihood profile for ϕ presented in Fig. S8, we find still find significant statistical evidence for susceptibility enhancement. Furthermore, the MLE of $\phi = 80$ is close to what we obtained from the original model.

S-3.2 Potential anomalies in data set II

Data set II spanned a period from the beginning of 2000 to the end of 2009. This included two potentially anomalous stretches. First, since the PCV was introduced in 2000, the early 2000s were potentially a period when pneumococcal vaccine uptake was increasing. Although, the pneumococcal pneumonia incidence are generally lower post-PCV compared to pre-PCV, we do not observe a strong trend in the data post 2000. Second, in the later part of 2009, the 2009 swine pandemic started. This led to anomaly in influenza incidences, which can be seen in the data. How might the results change, if one were to exclude these portions of the data? To address these issues, we present likelihood profiles for ϕ, based on the conditional likelihoods corresponding to several smaller periods. Since the likelihood function is a product of conditional likelihoods of each data point, likelihoods presented here are products of conditional likelihoods in the MLE that correspond to the chosen data. As seen in Fig. S9, the estimate of the susceptibility enhancement is remarkably similar even when only smaller subsamples of the data were considered, indicating that the signal of the enhancement does not completely reside on the early phase of the data (where vaccine uptakes may have been increasing), or the later phase (where the 2009 pandemic started).

S-3.3 Variation in influenza timing and detectability of interaction

Apart from variability in influenza peaks, variability in the timing of the influenza peaks may also contribute to our ability to detect interaction. This can be particularly informative if the timing of the influenza peaks are anomolous, as in some pandemics. What is perhaps worth noting is that in these non-pandemic years, the variability in the timing of the influenza peaks are within +/- 2 months. This variation in the timing of influenza tends to fall within the range of pneumococcal pneumonia peaks, the shape of which tend to be broader. Hence, in these non-pandemic years, the variation in timing of influenza peaks may not be as informative. As an illustration, we did some additional exploration with the simulation experiments similar to ones shown in Fig. 4 of the manuscript. Instead of changing the size of the influenza peaks in manufactured data, we varied their timing. As shown in Fig.S10, what we find is that variation in the timing of influenza peaks within (-/+ 8 weeks) by itself does not help identify the interaction.

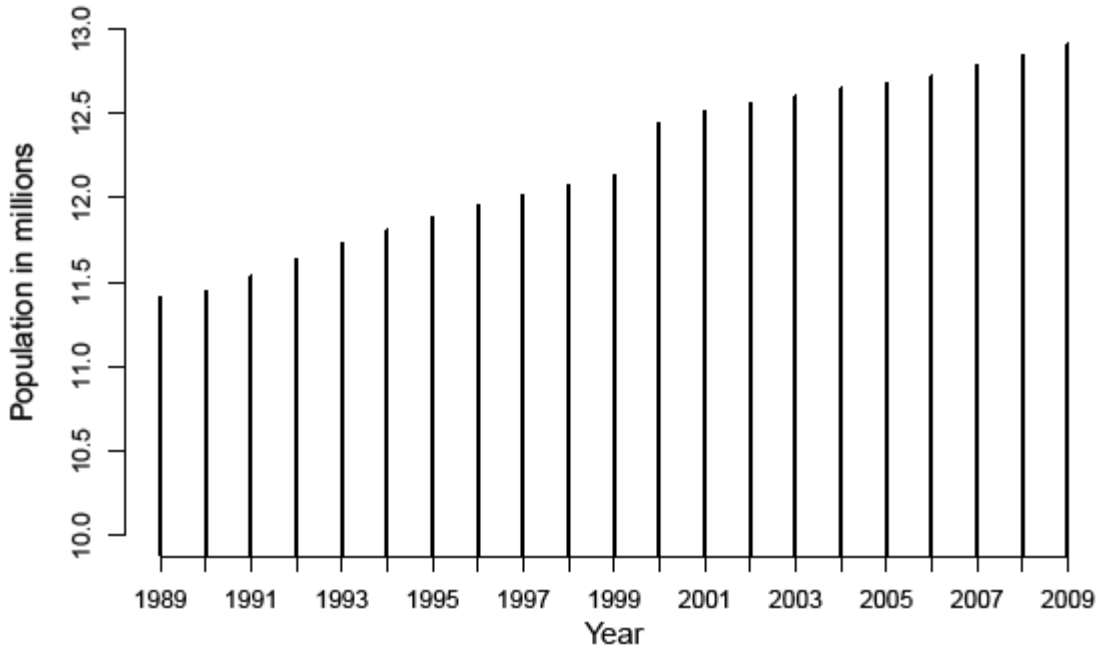

Figure S1: **Population of Illinois.**

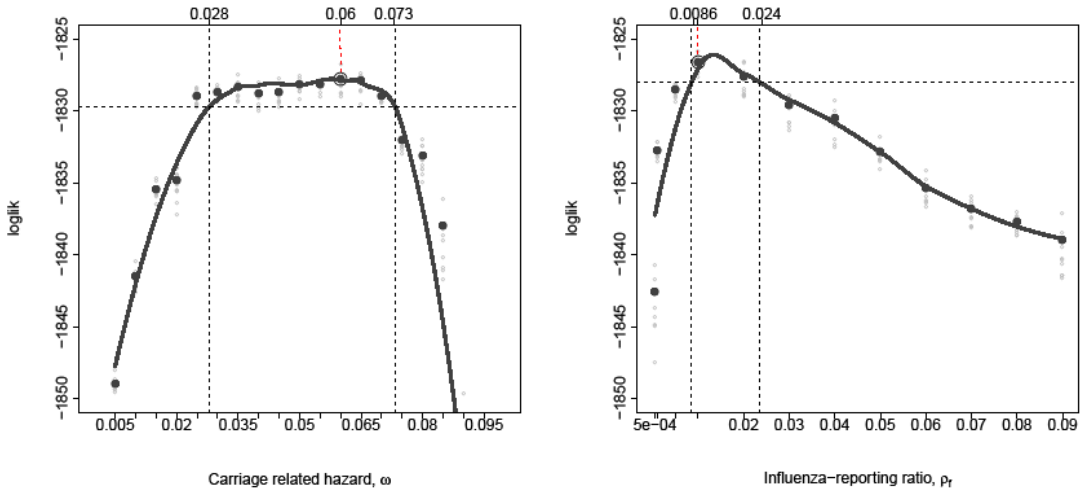

Figure S2: **Likelihood profiles for carriage-related hazard and influenza reporting ratio.** Shown are likelihood profiles for [Left] carriage-related hazard ω and [Right] influenza reporting ratio, ρ_F. The profiles are based on data set II. The vertical black dashed lines indicate 95% confidence interval, and the red dashed line shows the MLE.

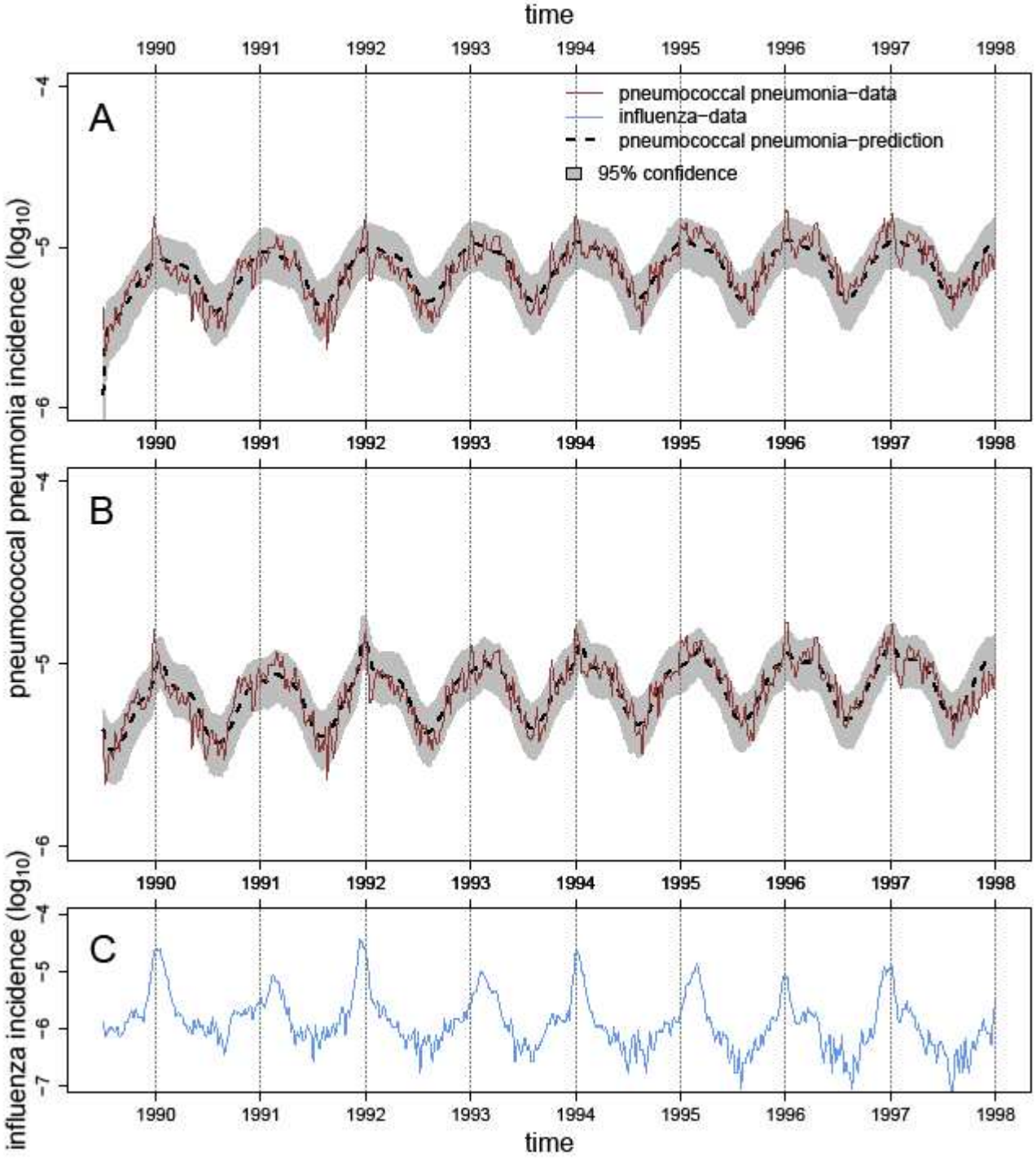

Figure S3: **Simulations from the models fit to data set I.** We compare the simulations from two fitted models with the data-(A) The null model, $\phi = 1$, and (B) The maximum likelihood estimate model (MLE-

model), with enhancement, $\phi = 115$. The models are simulated 1000 times to generate means and the confidence intervals. The covariate, influenza incidences are shown in (C).

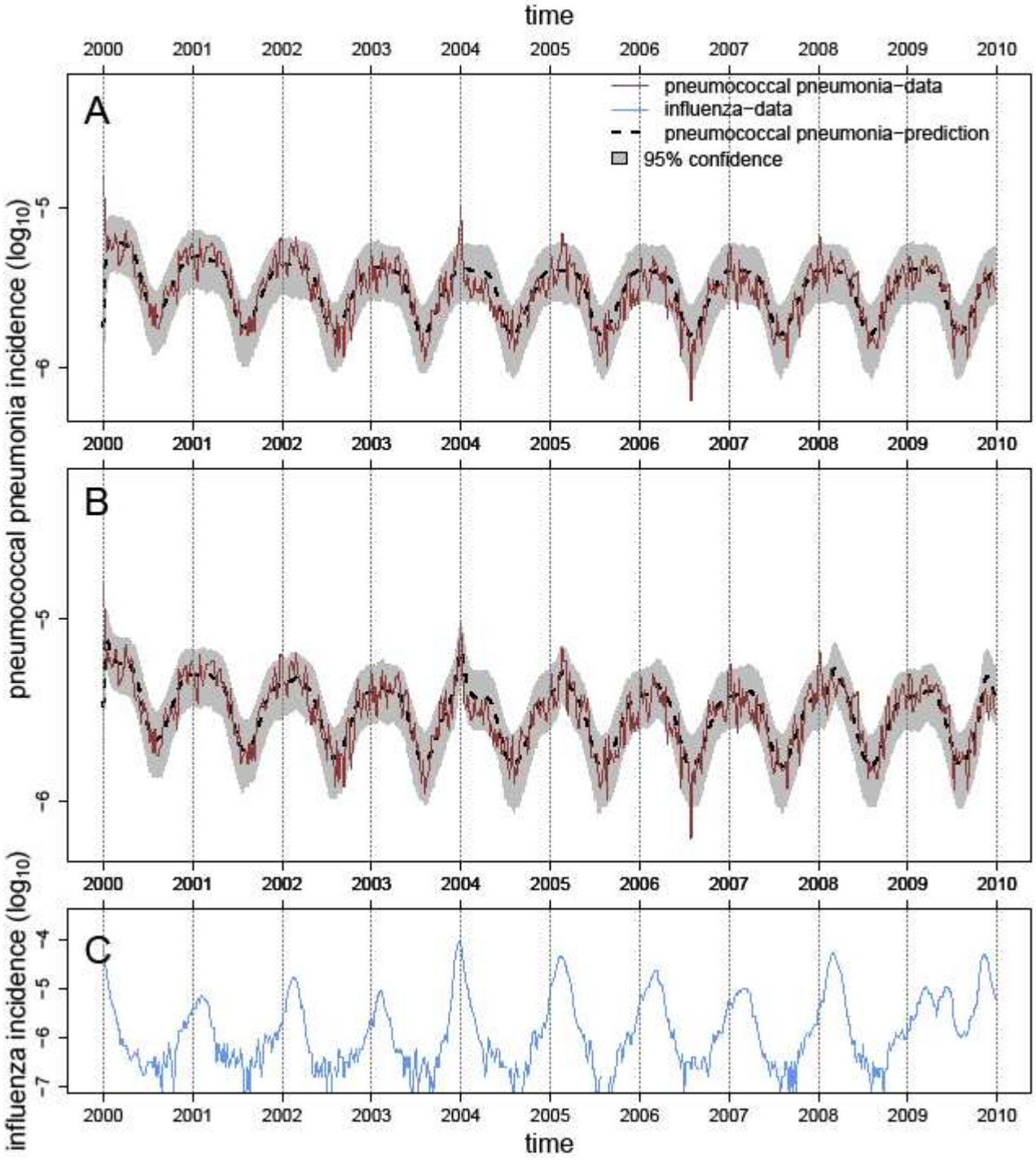

Figure S4: **Simulations of the models fit to data set II.** We compare the simulations from two fitted models with the data-(A) The null model, $\phi = 1$, and (B) The maximum likelihood estimate model (MLE-model), with enhancement, $\phi = 85$. The models are simulated 1000 times to generate means and the confidence intervals. The covariate, influenza incidences are shown in (C).

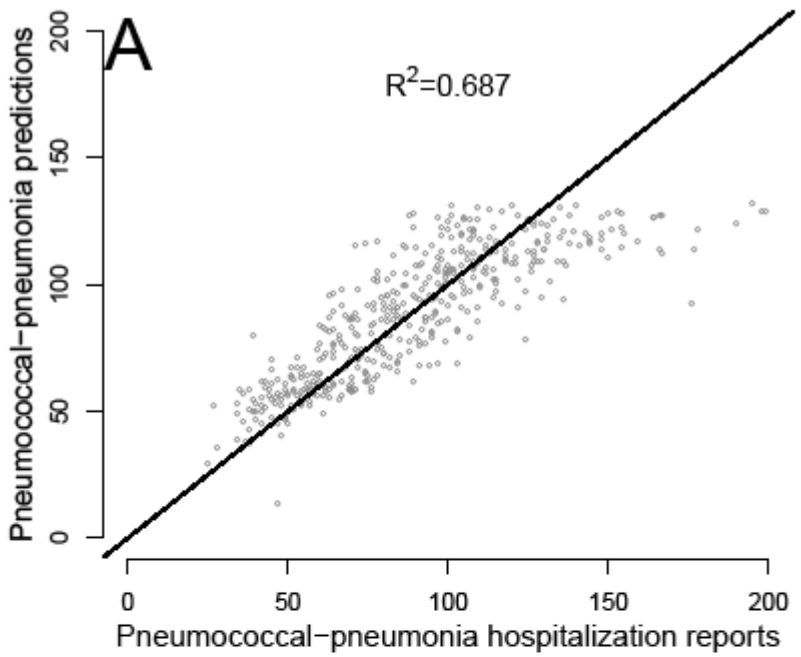
A
R^2=0.687
Pneumococcal−pneumonia predictions
Pneumococcal−pneumonia hospitalization reports
0
50
100
150
200

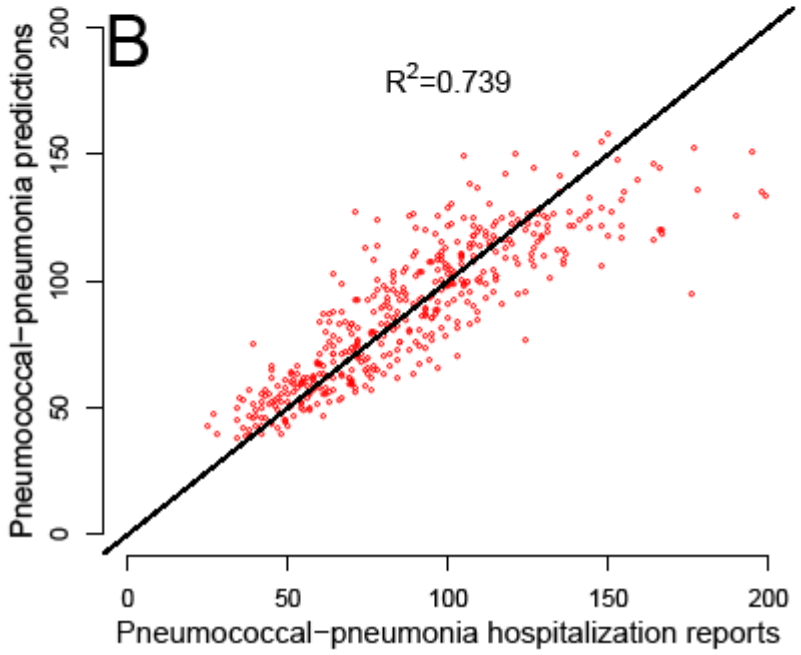
B
R^2=0.739
Pneumococcal−pneumonia predictions
Pneumococcal−pneumonia hospitalization reports
0
50
100
150
200

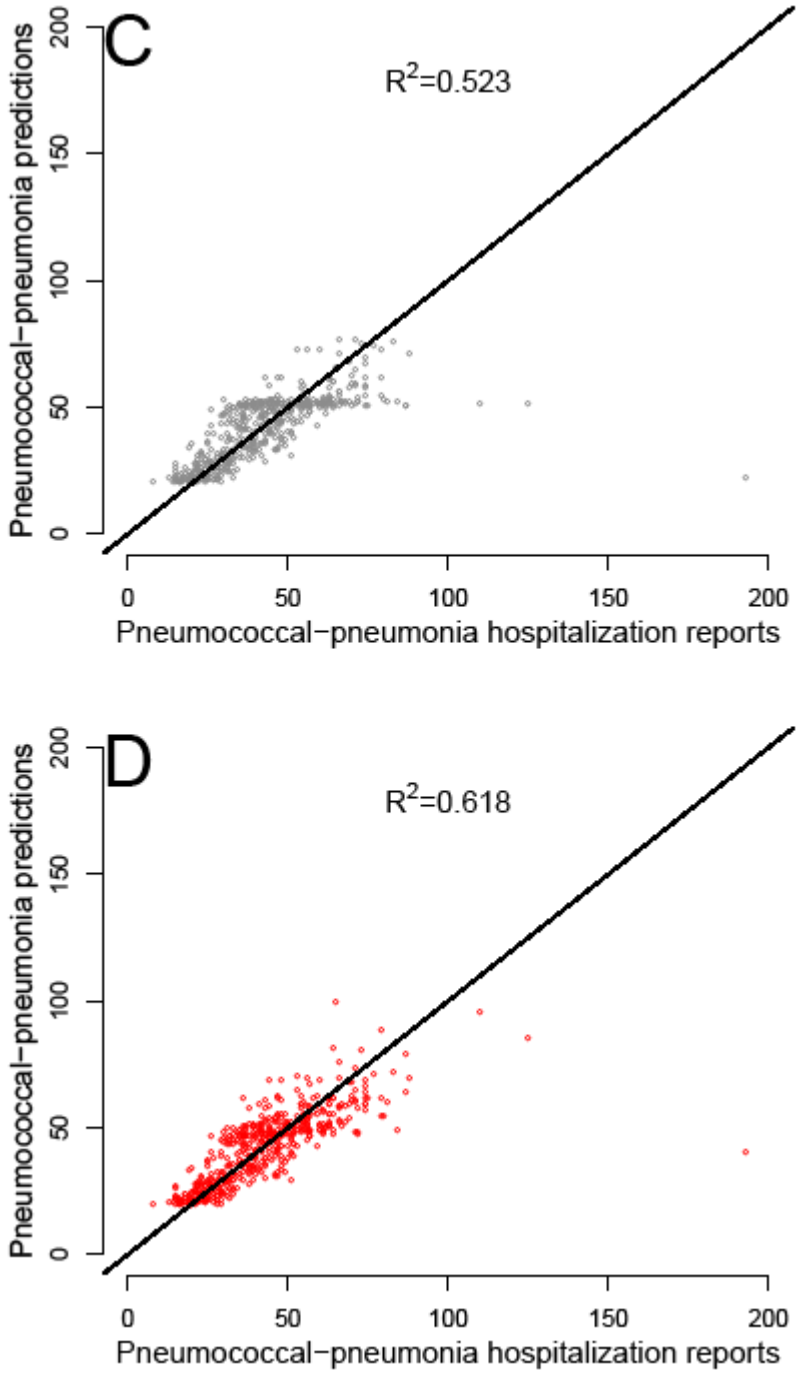

Figure S5: **Comparisons between predictions and the data.** Comparisons of the model predictions with (A & B) data set I, and (C & D) data set II. Predictions are based on means of 1000 simulations of (B & D) the MLE models and (A & C) the null models. Shown by R^2 are the fractions of variances in the respective data sets explained by the different models.

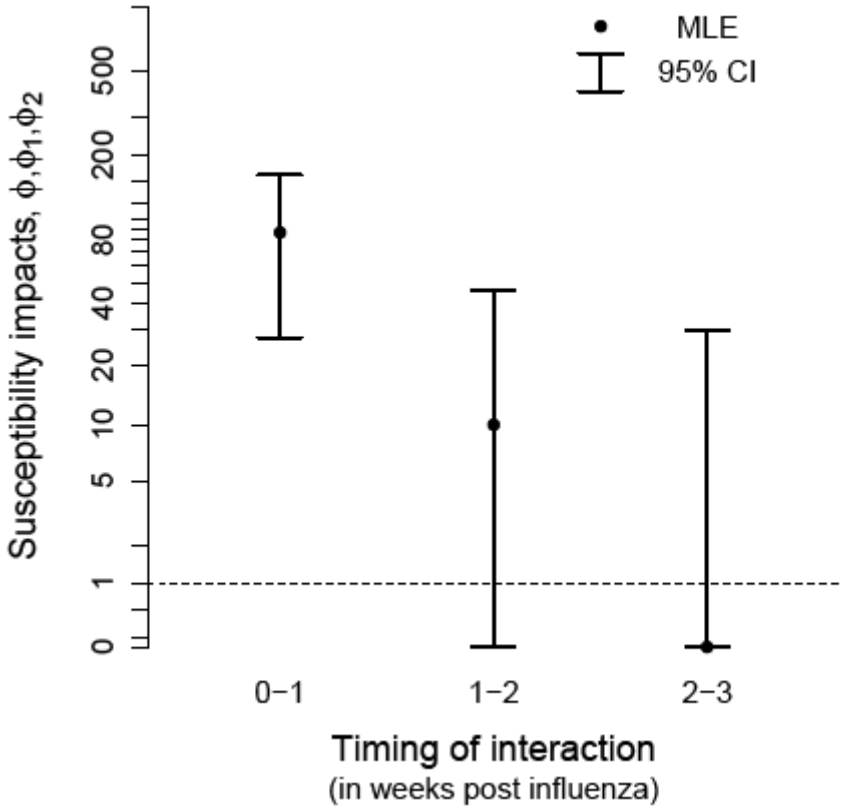

Figure S6: **Inference on the timing of the interaction.** We infer susceptibility impacts in pneumococcal pneumonia at different times post influenza infection in data set II. Estimates for susceptibility impacts are calculated in individuals up to 1 week post influenza, ϕ, between 1 and 2 weeks post influenza, ϕ_1, and between 2 and 3 weeks post influenza, ϕ_2. Black dots indicate the MLEs, and the vertical bars indicate the 95% confidence intervals. $\phi = 1$, $\phi_1 = 1$ and $\phi_2 = 1$ are the respective null models.

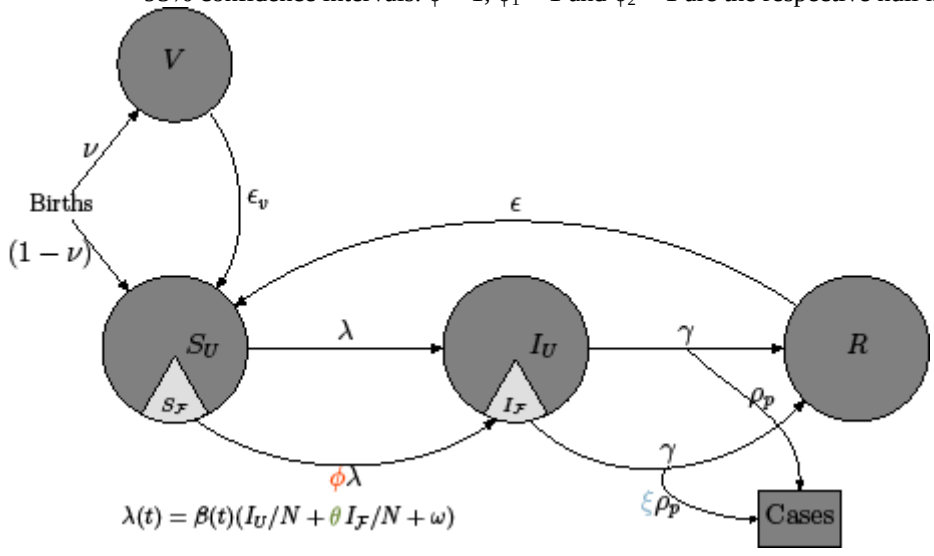

Figure S7: **Schematic representation of the alternative model with vaccine.** Here, we include a new compartment *V* of individuals that are currently protected against pneumococcal pneumonia due to vaccine-

derived immunity. We assume that ν fraction of the new-born individuals receive efficacious vaccine, and only the remaining (1−ν) fraction enter the susceptible class. We allow for waning of vaccine derived immunity at a per capita rate ε_v.

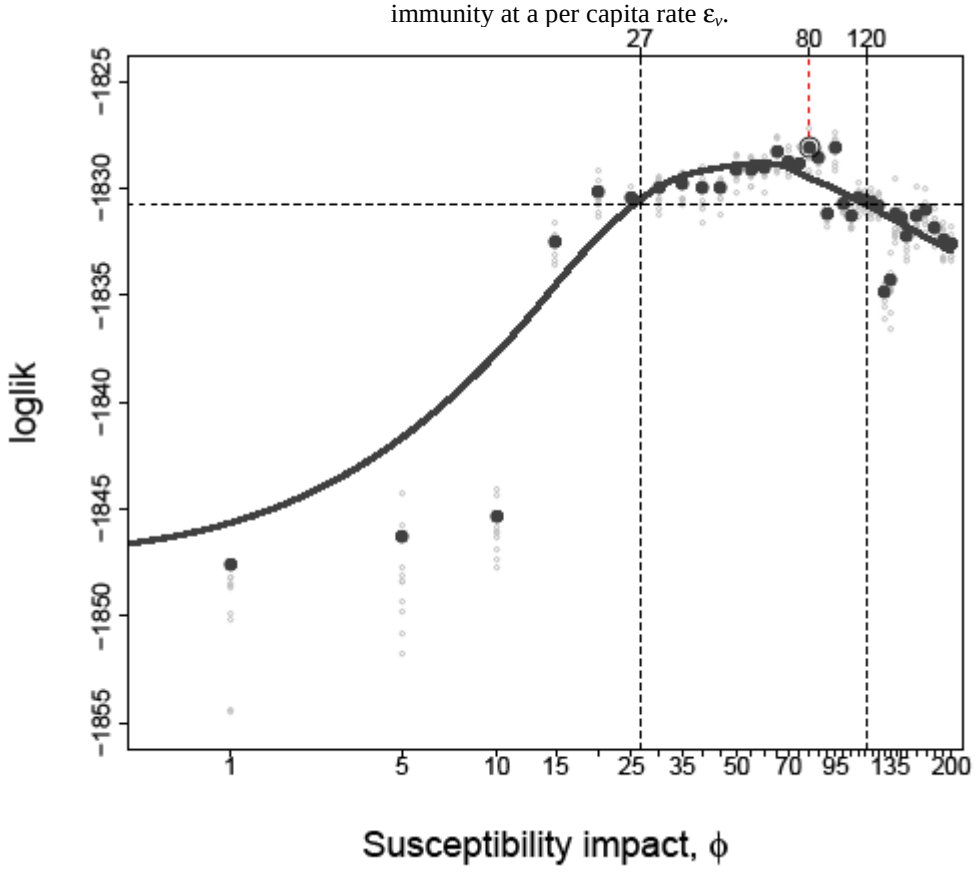

Figure S8: **The inference for influenza-pneumococcal pneumonia interaction using the alternative vaccine model.** We estimate hazard ratio ϕ in Illinois post-vaccine data (Data set III), using the likelihood framework. Likelihood for each profile point (filled black circle) is mean of the likelihoods in 10 replication (shown as open gray circles). All likelihoods are presented in natural log scale as log-likelihoods. The values of ϕ that fall between the two vertical dashed lines (between ~ 27 to ~ 120) are within the 95% confidence interval. The open red circle is the maximum likelihood estimate (ϕ = 80). These estimates are close to the estimates obtained using the original model [See the inset of Fig. 2H].

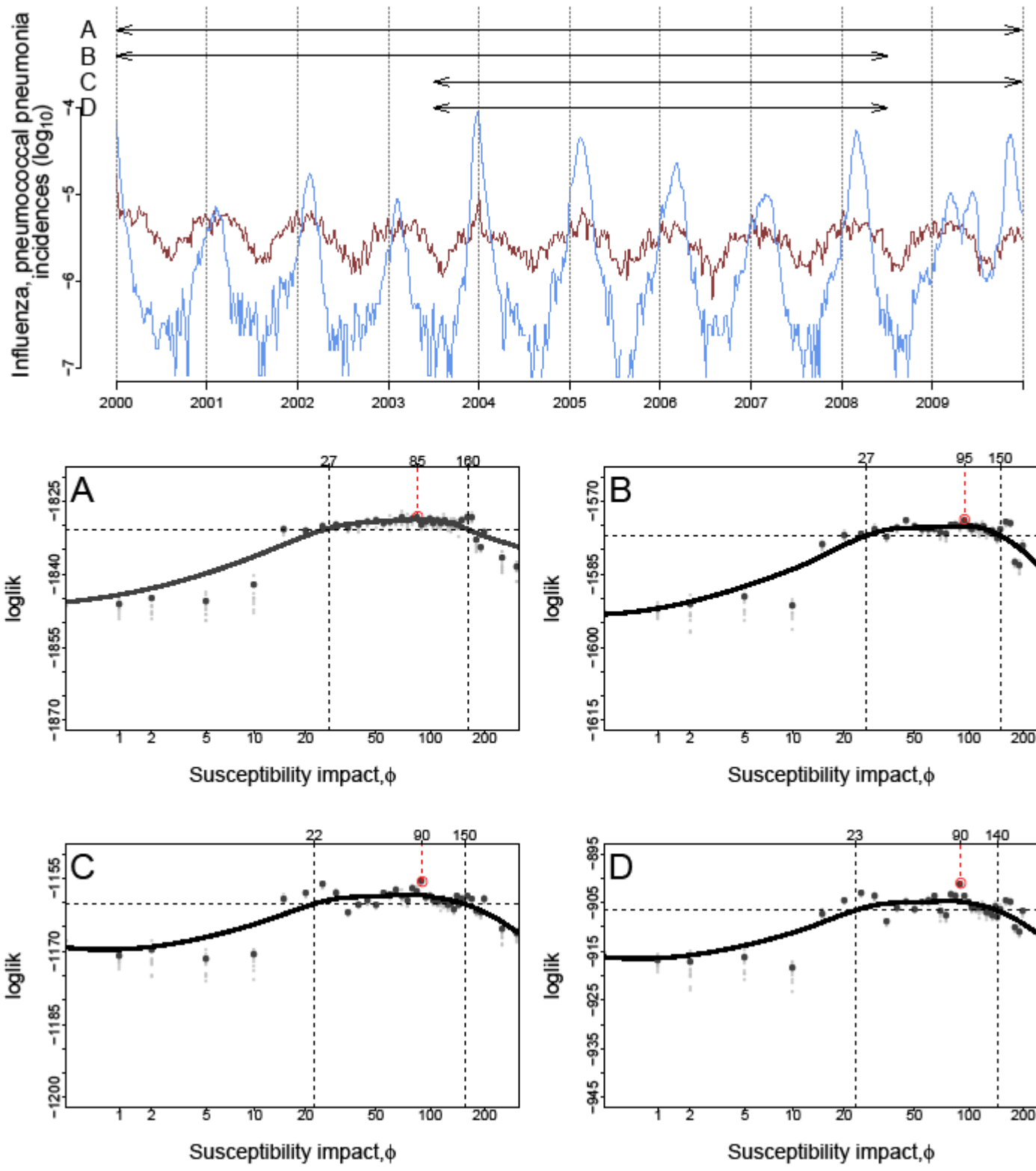

Figure S9: **Estimate of enhancement on various subsets of data set II.** We present the profiles of susceptibility impact, ϕ, on basis of subsets of the data set II. The range of data used are indicated in the top

panel. Likelihood profiles are based on product of conditional likelihoods in the MLE that correspond to the subset of the data.

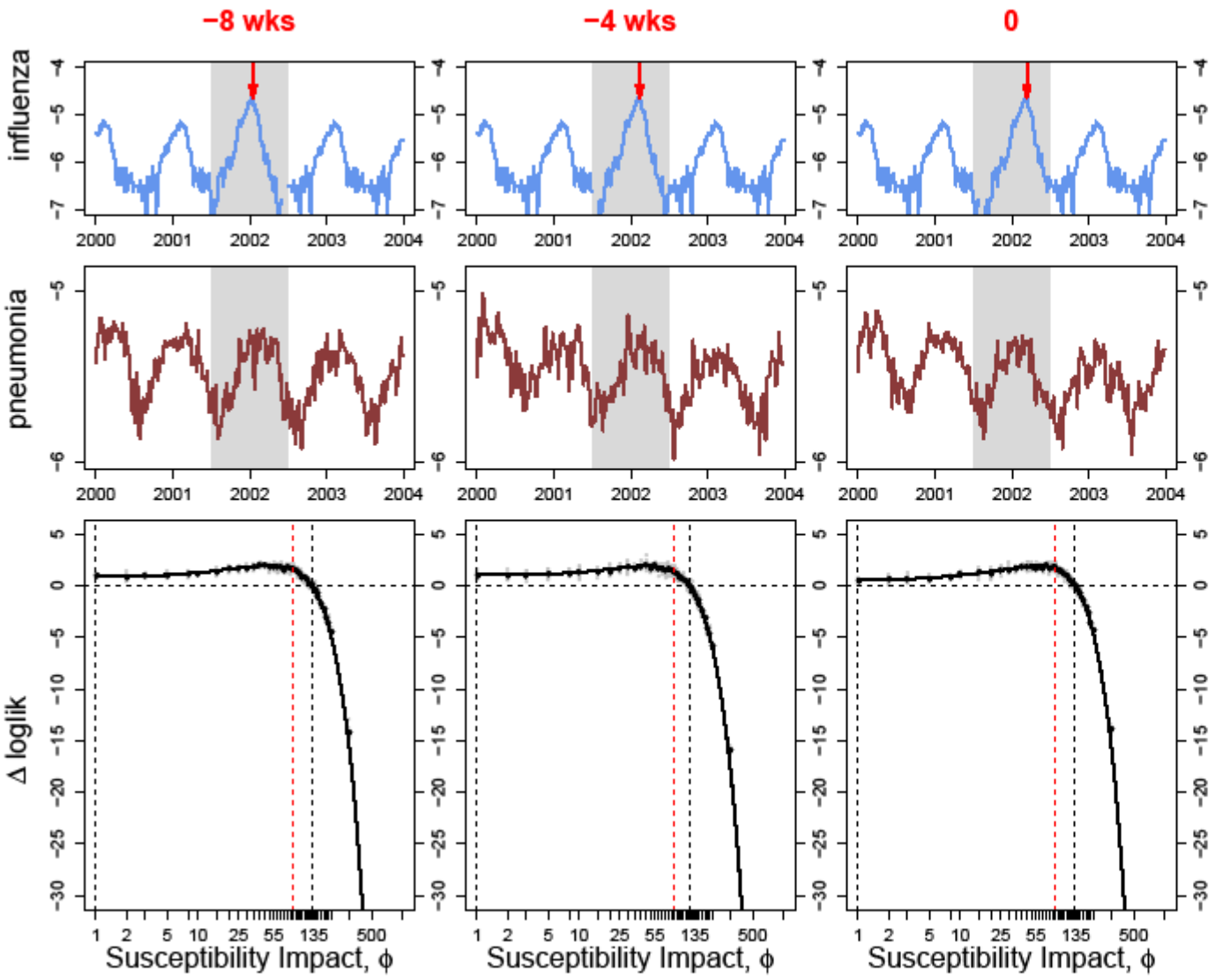

Figure S10: **The effect of timing of influenza peaks on detectability.** Plotted column-wise are inference tests performed on 5 sets of manufactured data sets. The data sets differ in that the third influenza peak is shifted by time intervals indicated at the top. Plotted in the top row are manufactured weekly influenza incidence reports (on a $\log_{10}$ scale). Plotted in middle row are simulated weekly pneumococcal pneumonia incidence reports (on a $\log_{10}$ scale) using the MLE-model, and influenza cases as covariates. And plotted in bottom row are likelihood profiles of the susceptibility, ϕ. The dashed red line is the actual value of interaction (ϕ = 85, MLE-model in data set II), and the values of ϕ between the two dashed black lines are within 95% confidence interval. Note that data with no shift is the same data as in scenario II of Fig 4 in the main text.

Algorithm parameter	**Description**	**Range**
Np	Number of particles	5000 - 10000
Nmif	Number of mif iterations	50 - 150

var.factor	Starting particle distribution	2 - 3
cooling.factor	Exponential cooling factor	0.95 - 0.99
ic.lag	Fixed-lag smoothing of initial-value parameters	2 - 4 years
rw.sd	Intensity of the random walk	0.005 - 0.02

Table S1: Parameters used in inference algorithm with their ranges.

Parameter	**Description**	Fit	**MLE**	
			(Estimated Range[†])	
			Data set I	**Data set II**
N	Population size	fixed/	covariate	covariate
		covariate		
μ	Host birth/mortality	fixed	0.02	0.02
	rate (year^{-1})			
γ	Host recovery	yes	76.7	90.5
	rate (year^{-1})		(66.34 – 109.0)	(81.44–115.3)
ε	Loss of immunity	yes	0.09	0.16
	rate (year^{-1})		(0.08–0.18)	(0.08–0.25)
ρ_F	Symptomatic ratio	yes	0.006	0.009
	(influenza)		(0.004–0.025)	(0.003–0.025[‡])
ρ_P	Symptomatic ratio	yes	0.024	0.001
	(pneumonia)		(0.014–0.033)	(0.001–0.002)
ω	Carriage-dependent	yes	0.004	0.03
	hazard		(0.002–0.004)	(0.027–0.064[‡])
β_1	Transmission rate	yes	8.38	18.07
	(1st seas. basis) (year^{-1})		(7.52 – 18.49)	(8.92 – 18.43)
β_2	Transmission rate	yes	8.21	17.54
	(2nd seas. basis) (year^{-1})		(7.74 – 17.29)	(8.44 – 17.54)
β_3	Transmission rate	yes	8.59	20.92
	(3rd seas. basis) (year^{-1})		(7.93 – 17.51)	(9.95 – 21.55)
β_4	Transmission rate	yes	3.84	7.08
	(4th seas. basis) (year^{-1})		(3.66 – 8.45)	(3.42 – 7.21)
β_5	Transmission rate	yes	4.55	8.48

	(5th seas. basis) (year^{-1})		(4.14 – 10.07)	(3.99 – 8.69)
β_6	Transmission rate	yes	8.23	17.32
	(6th seas. basis) (year^{-1})		(7.60 – 17.12)	(8.20 – 17.46)
β_{sd}	Std. deviation of	yes	0.027	0.027
	extra-demographic noise		(0.024 – 0.027)	(0.026–0.029)
c	Observation model	yes	0.83	0.77
	scalar		(0.77 – 0.89)	(0.7 – 0.78)
ϕ	Susceptibility	yes	115	85
	Enhancement		(70–200)	(30–160)
$S(0)$	Initial susceptible	yes	0.46	0.44
	fraction		(0.45–0.56)	(0.22–0.63)
$I(0)$	Initial infectious	yes	1.5×10^{-4}	2.5×10^{-5}
	fraction		($0.82–2.5\times10^{-4}$)	($1.2–3.9\times10^{-5}$)
$R(0)$	Initial recovered	fixed	0.54	0.56
	fraction		(0.44–0.55)	(0.37–0.78)

Table S2: Model parameters and their estimated range for epidemiology of pneumococcal pneumonia. † Estimated range for each parameter shown in this table corresponds to the respective range observed while calculating 95% confidence interval for φ. Note that the ranges presented here are not necessarily 95% confidence intervals for each parameter, except for parameter φ, for which the 95% confidence interval was calculated. ‡ Please refer to profiles shown in Fig. S2 for accurate 95% confidence intervals.